HortScience 58(9):1057–1067. 2023. https://doi.org/10.21273/HORTSCI17300-23

Simulation and Experiment on the Falling Pattern of Fresh Tea Leaves Based on Discrete Elements

Xu Zhang and Xinyu Zhu

Intelligent Manufacturing and Elevator Institute, Huzhou Vocational & Technical College, Huzhou, 313000, China

Keywords. discrete meta-particles, EDEM simulation, motion morphology

Abstract. **Tea [*Camellia sinensis* (L.) O. Ktze] is loved by people all over the world. For accurate simulation of the falling motion characteristics of fresh tea leaves, this study took one bud and two leaves of fresh tea leaves as the research object, and established a 1:1 three-dimensional (3D) model of fresh tea leaves by using 3D scanning and reverse modeling technologies. The 3D fresh tea leaves model was filled with discrete element particles, and the motion pattern of fresh tea leaves within a certain distance from the ground was simulated. The falling shape of fresh tea leaves was captured by the high-speed camera to verify the established model. By adjusting parameters to optimize the model, it was concluded that the simulation was in good agreement with the test, indicating that the established model is correct. According to the simulation, the fall analysis of four kinds of fresh tea leaves, A, B, C, and D, placed on the transmission belt was carried out. The distance between the transmission belt and the ground was 80 cm. Among them, A leaves were 45 cm, B leaves were 55 cm, C leaves were 55 cm, and D leaves were 65 cm away from the ground. The movement characteristic of fresh tea leaves is vertical on the ground. In different positions from the ground during the falling process, it was found that all kinds of fresh tea leaves were rotated around the stalk axis and the middle part of the fresh tea leaves. In conclusion, the establishment of a discrete element model of fresh tea leaves' movement morphology and the analysis of movement morphology during the falling process laid a theoretical foundation for the study of air suction sorting of fresh tea leaves in the later period.**

With the rapid advancement of agricultural modernization, the level of agricultural mechanization in China is constantly improving, and machinery and tools are gradually developing in the direction of intelligence and efficiency (Dong et al. 2017). Pneumatic conveying has begun to be widely used in a variety of agricultural equipment, such as seeding, fertilization, and harvesting machinery (Qi et al. 2016; Wang et al. 2015; Xing et al. 2019). At the same time, with the gradual rise of labor costs and the aging population trend, tea-leaf picking has become an important factor restricting the development of the tea industry, and machine tea picking will gradually become important (Tang et al. 2015). At present, the cost of picking fresh leaves with a reciprocating tea-cutting machine is low and the yield is excellent; however, dealing with the components of fresh tea leaves in tea picking by reciprocating machine are more complex. These include, for example, picking leaves, bud heads, one bud, one leaf, one bud and one leaf, one bud and two leaves, one bud and three leaves, damaged buds and leaves, and so on. Direct processing will affect the quality and price of late tea, so the sorting and classification of fresh tea leaves are particularly important, but the air suction sorting method focuses on the movement shape of fresh tea leaves.

In recent years, with the wide application of the discrete element method in the simulation analysis of agricultural granular materials, scholars have analyzed corn stalk particles (Li et al. 2015; Wang et al. 2018, 2021), stalk broken particles (Liao et al. 2020), soil particles (Wang et al. 2017), fertilizer particles (Peng et al. 2018; Wen et al. 2020), potato particles (Liu et al. 2018; Wang et al. 2017), rice particles (Lu et al. 2018; Yuan et al. 2018), spinach root (Li et al. 2021), for example. The discrete element model of agricultural materials with relatively simple appearance is thus established and simulated. On this basis, existing equipment is continuously optimized and upgraded, and new equipment is developed. In recent years, scholars in China and elsewhere have attempted to establish and simulate the discrete element model of fresh tea leaves. For example Lv et al. (2022), based on the discrete element method of EDEM software, optimized the classification parameters of vibrating classifier for fresh tea leaves by machine. Li et al. (2019) adopted a spherical particle polymer filling model and contact mechanics model for fresh leaves of various grades and conducted a sorting simulation in EDEM. Wang (2020) established a similar discrete element model of fresh tea leaves through particle accumulation and conducted relevant simulation studies. However, it has been shown that there are differences between discrete element simulation particles and real models, and these will directly affect the accuracy and results of the simulation. Therefore, the establishment of a discrete element model of a 1:1 multiscale machine for picking fresh tea leaves has significance for the accuracy of discrete element simulation.

We considered "one bud and two leaves" of machine-picked fresh tea leaves as the simulation and test objects and conducted inverse modeling of 3D scanning of fresh tea leaves, discrete element simulation, and experimental research. We used high-speed cameras to track the falling morphology of fresh tea leaves and compare the results and thus verify the feasibility of the multiscale simulation test of the falling morphology of fresh tea leaves by machine-picked tea leaves based on discrete elements. According to the test results, the discrete element model was refined, laying a theoretical foundation and discrete element model for the separation of fresh tea leaves by air suction.

Materials and Methods

Fresh tea leaves. The fresh tea leaves used in the experiment were one bud and two leaves, and the geometric size of the long axis of the material was randomly distributed between 55 and 80 mm. The mass of one bud and two leaves was measured by scientific balance, and an average value was obtained. The mass was 0.21 g.

3D scanning system and high-speed camera system. The 3D scanning system adopted in this research included the OKIO noncontact optical 3D scanner (jointly developed by Beijing Tianyuan 3D Technology Co., Ltd. and Tsinghua University with independent intellectual property rights), automatic turntable, and computer. The scanners mainly included industrial 5-megapixel cameras and raster-generating devices, with scanning accuracy of 0.005 to 0.015 mm and average sampling point distance of 0.04 to 0.016 mm, as shown in Fig. 1. The high-speed camera system captured and recorded the falling motion patterns of fresh tea leaves and verified the discrete element model in this study. The high-speed camera system consists of a high-speed camera and a computer. The resolution of the camera is 1920 × 1080, and the frame number is 2150 frames per second.

Discrete element simulation method. The discrete element method was used to simulate multiscale motion characteristics of fresh tea leaves falling from the conveyor belt. The basic model selected for this study was the Hertz–Mindlin (No Slip) model, which is accurate and efficient in force calculation. In this model, the normal force component is based on Hertzian contact theory, and the tangential force model is based on Middlin–Deresiewicz's research theory. Both the normal force and tangential force have damping components, which are related to the damping coefficient and recovery coefficient. The tangential friction force complies with Coulomb's law of friction. Rolling friction independent directional constant torque model through contact (Di Renzo and Di Maio 2004; Oka et al. 2005; Potyondy and Cundall 2004; Sakaguchi 1993). For the normal force F_n, the expression is as follows:

Received for publication 12 Jun 2023. Accepted for publication 6 Jul 2023.
Published online 18 Aug 2023.
This work was supported by the general scientific research project of Zhejiang Education Department (No. Y202250526).
Xu Z. is the corresponding author. E-mail: z_xu1987@163.com.

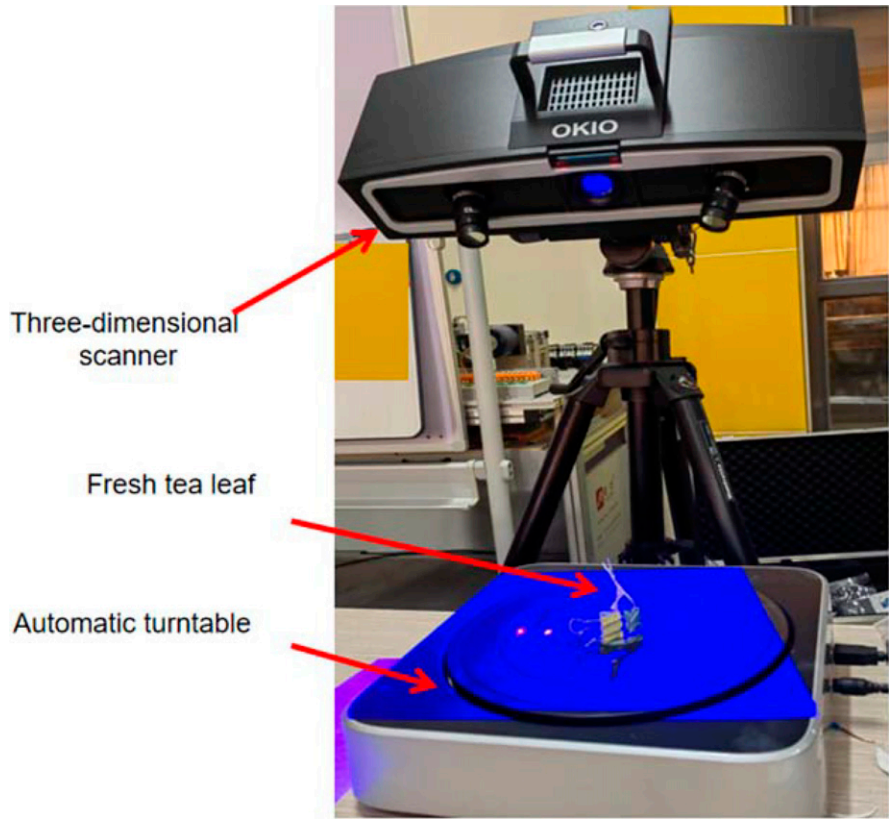

Fig. 1. Three-dimensional scanner.

$$F_n = \frac{4}{3}E^*\sqrt{R^*}\delta_n^{\frac{3}{2}} \quad [1]$$

For the equivalent Young's Modulus E^*, the equivalent radius R^* is defined as

$$\frac{1}{E} = \frac{\left(1-v_i^2\right)}{E_i} + \frac{\left(1-v_j^2\right)}{E_j} \quad [2]$$

$$\frac{1}{R^*} = \frac{1}{R_i} + \frac{1}{R_j} \quad [3]$$

E_i, v_i, R_i, and E_j, v_j, and R_j, are Young's Modulus, Poisson ratio, and Radius of each sphere in contact. Additionally, there is a damping force, F_n^d, given by

$$F_n^d = -2\sqrt{\frac{5}{6}}\frac{\ln e}{\sqrt{\ln^2 e + \pi^2}}\sqrt{2E^*\sqrt{R^*\delta_n}m}\ v_n^{\vec{rei}} \quad [4],$$

where m is the equivalent mass, $v_n^{\vec{rei}}$ is the normal component of the relative velocity, β and S_n is the normal stiffness, and e is the recovery coefficient. For tangential forces F_t, the expression is

$$F_t = -8G^*\sqrt{R^*\delta_n}\delta_t \quad [5],$$

where G^* is equivalent shear modulus, δ_t is tangential overlap quantity.

For tangential damping force F_τ^d, the expression is

$$F_\tau^d = -2\sqrt{\frac{5}{6}}\frac{\ln e}{\sqrt{\ln^2 e + \pi^2}}\sqrt{2E^*\sqrt{R^*\delta_\tau}m}\ v_\tau^{\vec{rei}} \quad [6]$$

For simulation, rolling friction is important, considered by applying a torque to the contact ground, the expression is

$$\tau_i = -u_r F_n R_i w_i \quad [7],$$

where, u_r is the rolling friction coefficient, R_i is the distance from the contact point to the center of mass, and w_i is the unit angular velocity vector of the object at the contact point. The Bonding V2 model in EDEM should also be loaded because fresh tea leaves are flexible sheets and have certain bending deformation behavior. The bonding force/torque in the model is complementary to the basic contact model. Because the bonds involved in this model can function when the particles are no longer in physical contact, the contact radius should be set higher than the actual radius of the sphere, and the bond will break when the normal and tangential shear stresses exceed a certain predetermined value. The weight of fresh tea leaves is relatively light, and thus it is necessary to consider the influence of air resistance during falling on the motion state of fresh tea leaves. The air resistance contact model was added to EDEM. The resistance model was applied to fresh tea leaves particles, and the direction of movement was opposite to that of fresh tea leaves.

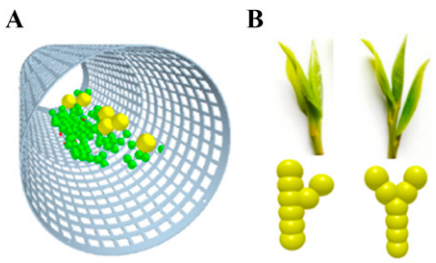

Fig. 2. The discrete element model of fresh tea leaves was established by various scholars. (**A**) Single pellets instead of fresh tea leaves. (**B**) A multipellet combination replaces fresh tea leaves.

Results

Inverse modeling of fresh tea. Fresh tea leaves are flexible, and it is difficult to establish 3D models for them because there are certain deviations in contour and thickness. At present, the models of fresh tea leaves established by scholars based on discrete elements are mostly similar in geometry; for example, fresh tea leaves were replaced with spherical particles or with similar buds, leaves, and leaves composed of stacked spheres, as shown in Fig. 2 (Li et al. 2019; Wang 2020). Several studies have shown that the closer the discrete element simulated particle is to the actual object, the higher the accuracy of the simulation.

A 3D scanner was used to conduct 3D scanning of fresh tea leaves picked by a multiscale machine. After scanning, the scanned point cloud image was repaired using Geomagic Wrap software, and then reverse modeling was performed on the repaired point cloud image using Geomagic Design X software. A multiscale tea fresh leaf model of one bud, two leaves, one bud, one leaf, and single leaf was established, but this study focuses on one bud and two leaves of fresh tea.

Discrete element particle filling. The 1:1 fresh tea leaves model was imported into the EDEM discrete element software. The fresh leaves of one bud and two leaves were filled with particles. A total of 2384 particles were filled, and the average pellet radius was 0.162 mm. By adjusting the density of fresh tea leaves within the allowable range, it was determined that the mass of the model after the fresh tea leaves of one bud and two leaves filled was 0.2042 g, which was similar to the 0.21 g measured by the test. Moreover, the particle filling was all within the model contour, and the filling rate was greater than 97.6%, as shown in Fig. 3.

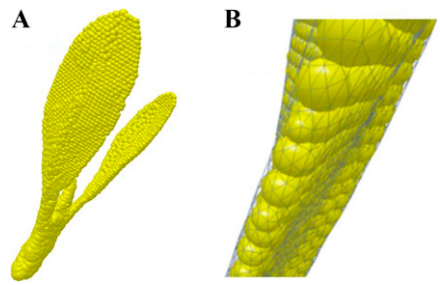

Fig. 3. Tea leaf model discrete element particle filling. (**A**) Discrete element particle filling model of fresh leaves of one bud and two leaves of tea. (**B**) The filled discrete particles are arranged in a three-dimensional model.

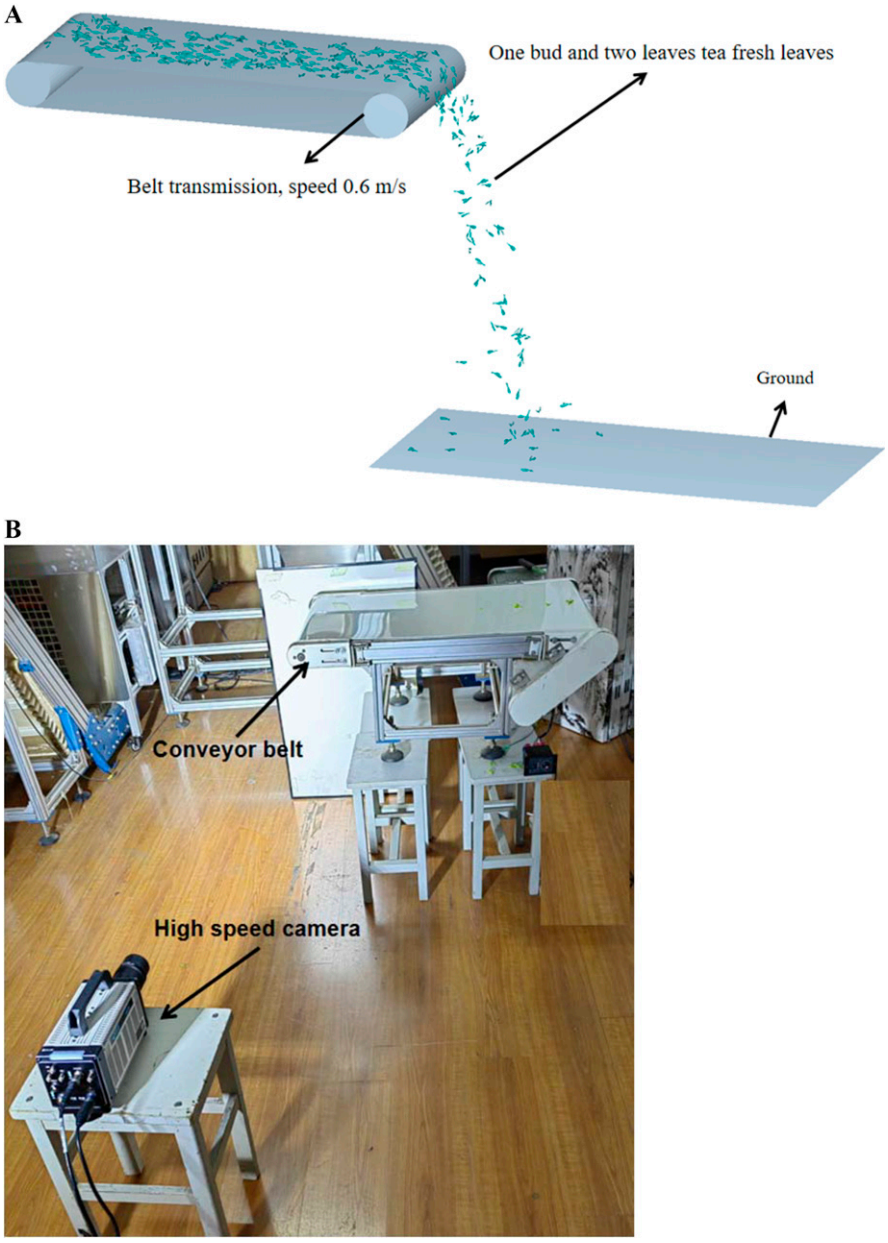

Fig. 4. (**A**) Discrete element simulation and test bench of fresh tea leaves based on EDEM. (**B**) Discrete element simulation of the falling movement pattern of fresh tea leaves. Tea leaf falling motion from the test bench.

Physical parameters of fresh tea. Due to the influence of tea tree growth, environment, and other factors, fresh tea leaves of the same variety have different outline shapes, and their bud and leaf lengths are different. In this study, 200 samples of one bud and two leaves of fresh tea leaves were selected to measure the size of fresh tea leaves. It was found that the bud length of one bud and two leaves ranged from 10 to 15 mm, and the leaf length ranged from 20 to 35 mm. The toughness, ductility, and mechanical properties of fresh tea leaves were tested by a texture analyzer. Through the compression test on the stem of fresh tea leaves, the average elasticity modulus and shear modulus of tea leaves were measured at 9.3 and 3.3 MPa, respectively.

EDEM model parameter setting. The falling movement pattern of fresh tea leaves with one bud and two leaves was simulated. The leaves fall on the conveyor belt, and the air resistance when the leaves fall is ignored in the simulation. The conveyor belt was 0.8 m from the ground, 0.75 m long, and 0.5 m wide, with a transmission speed of 0.6 m/s. The particle factory in the simulation process was in the dynamic generation mode, with a total of 600 pieces generated and a production capacity of 200 pieces per second. Because the size of the fresh leaves is different, the size distribution of leaves can be set in EDEM, and the setting modes are fixed, log-normal, normal, and random. In this study, the fixed size distribution of fresh tea leaves was adopted, and leaves with the same shape and size as the discrete element model were selected for the test. The writing frequency of the simulation data was set to 0.01 s. The simulation mesh size was set to three times the minimum particle radius, and the total simulation time was 4 s.

Simulation and verification of falling movement morphology of fresh tea leaves based on EDEM. Through the discrete element simulation, the particle factory generated a bud and two leaves of fresh tea at 0.1 m above the belt, and the belt transported tea to the edge of the belt at a speed of 0.6 m/s; the fresh tea leaves then fell at 0.8 m above the ground. A test bench identical to the discrete element simulation model was built, and a high-speed camera was used to photograph the falling motion pattern of fresh tea leaves. The same angle of view of simulation and test at every 0.1-m interval from the ground was selected for verification, and the motion pattern of fresh tea leaves falling at different heights was observed (Fig. 4).

Discrete tea particles with the same shape as those placed before the fall of fresh tea leaves were selected to verify the accuracy of the established model. The falling pattern of fresh tea leaves was captured by high-speed cameras at critical points of the falling movement: 0.7, 0.6, 0.5, 0.4, 0.3, 0.2, and 0.1 m from the ground. Comparison was made with the discrete element simulation results at the same distances (Fig. 5).

Figure 5A shows the critical point where fresh tea leaves are about to fall. It is shown by high-speed camera and simulation that the tea roots are all facing downward at the critical point of fall. Figure 5B shows the point where fresh tea leaves fall 0.7 m from the ground. The comparison between the test and the simulation shows that the fresh tea leaves have a rotating trend and are parallel to the ground, and the simulation and the test have the same movement trend. Figure 5C shows the place where fresh tea leaves fall 0.6 m from the ground. Compared with the test and simulation, the leaves here change from parallel to the ground at 0.7 m from the ground to the "partial vertical" downward movement of tea roots. Figure 5D–H shows the drop distance of 0.5 to 0.1 m of the leaves from the ground. The comparison between the test and the simulated tea leaves showed that in the same environment, the movement trend of fresh tea leaves was the same as that of the discrete element simulated tea leaves, with the stem diameter of fresh tea leaves moving downward and the page moving upward. In conclusion, through the discrete element simulation and the verification of the falling motion patterns of fresh tea leaves at different distances from the ground, agreement between the model and the test was greater than 95%, indicating the accuracy of the model. Therefore, the falling motion patterns of fresh tea leaves in different placement forms can be analyzed with this model, laying a foundation for research on the mechanism of fresh tea leaf sorting by air suction in the later stage.

Discussion

The location of fresh tea leaves on the transmission belt was selected, and we distinguished them according to the orientation of

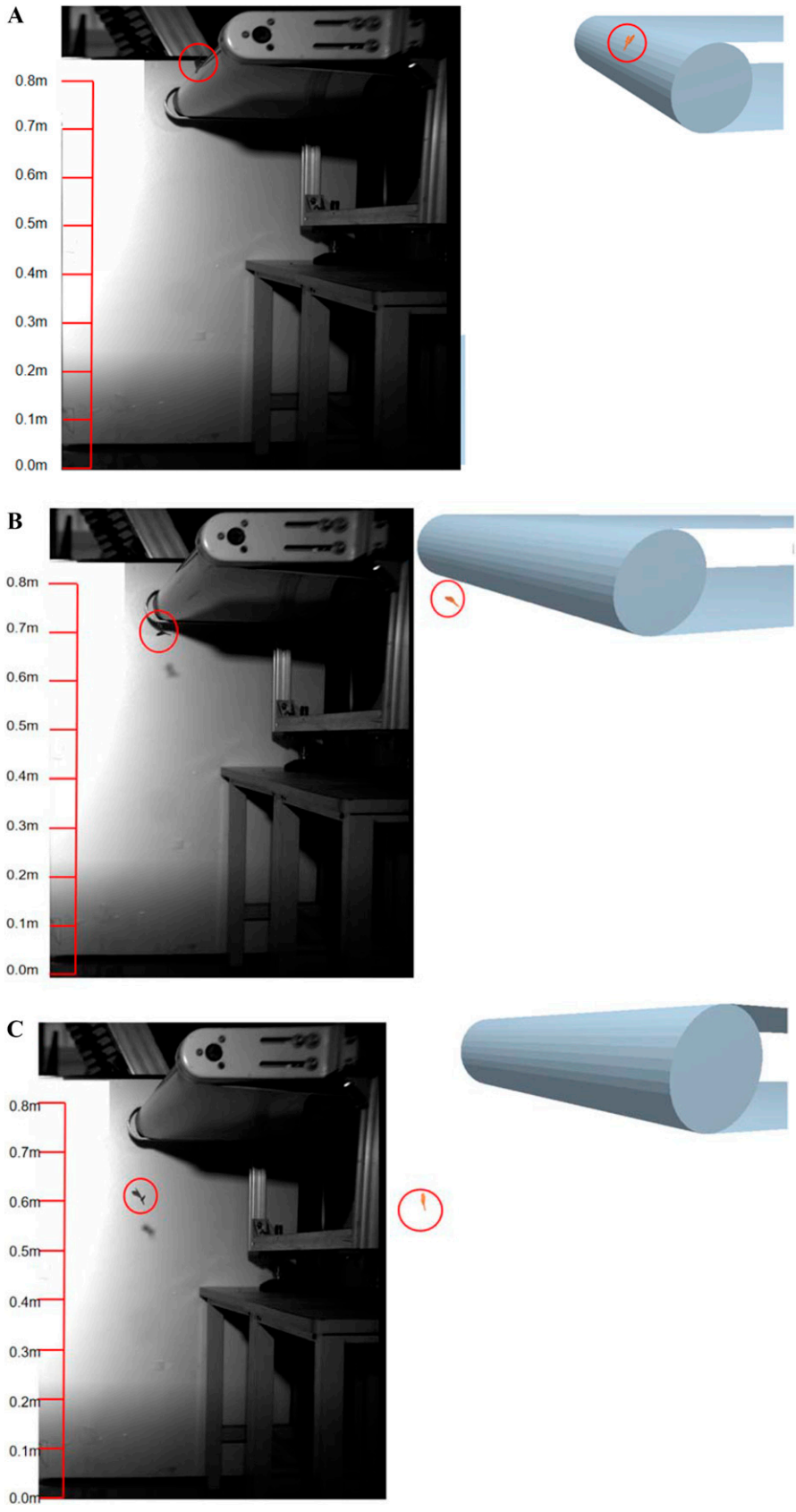

Fig. 5. The falling bench test of fresh tea leaves verified the discrete element simulation. (**A**) The state of fresh tea leaves before they are about to fall from the conveyor belt is shown: fresh tea leaves falling from the conveyor belt at (**B**) 0.7, (**C**) 0.6, (**D**) 0.5, (**E**) 0.4, (**F**) 0.3, (**G**) 0.2, and (**H**) 0.1 m from the ground.

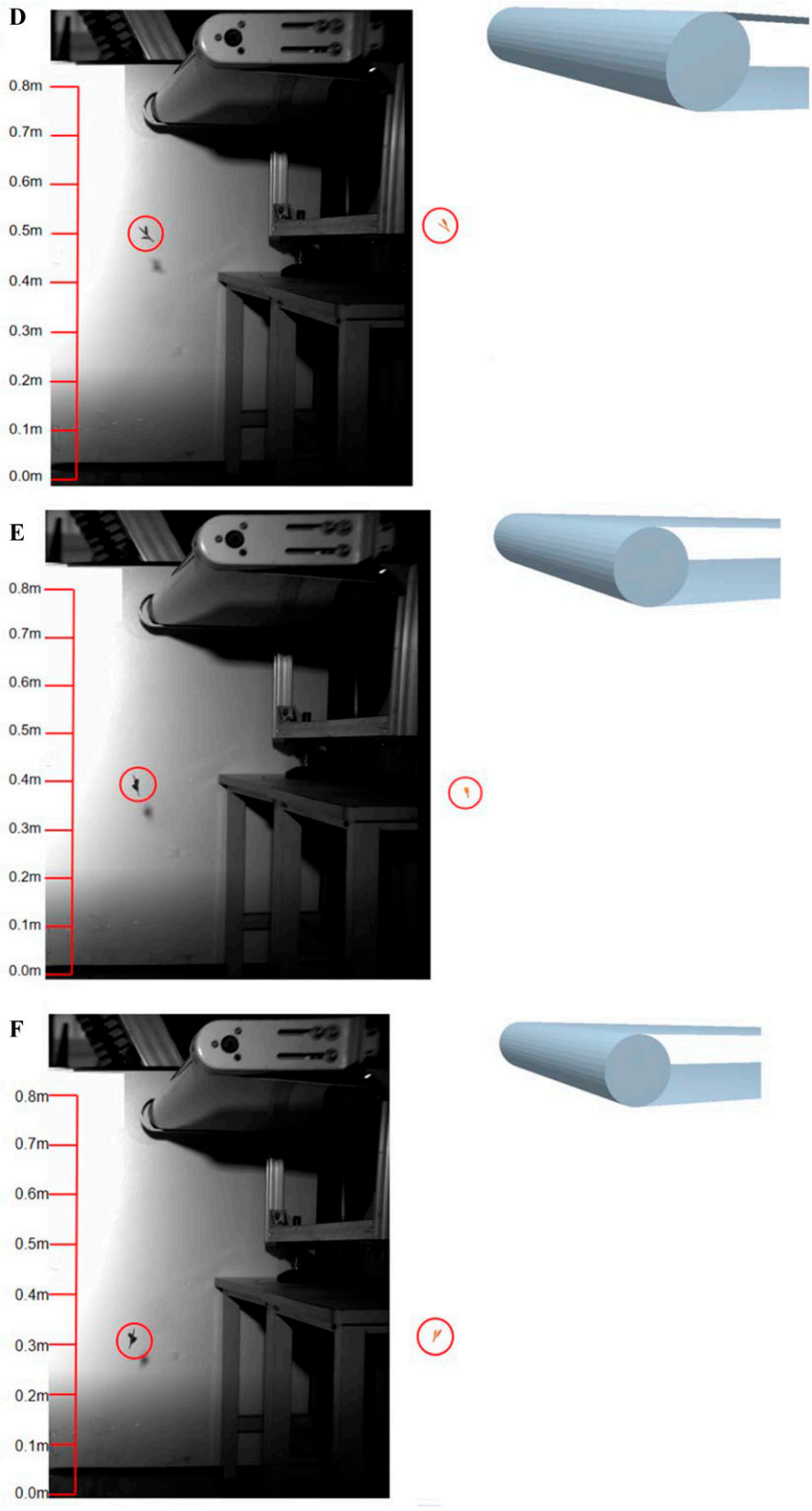

Fig. 5. (*Continued*)

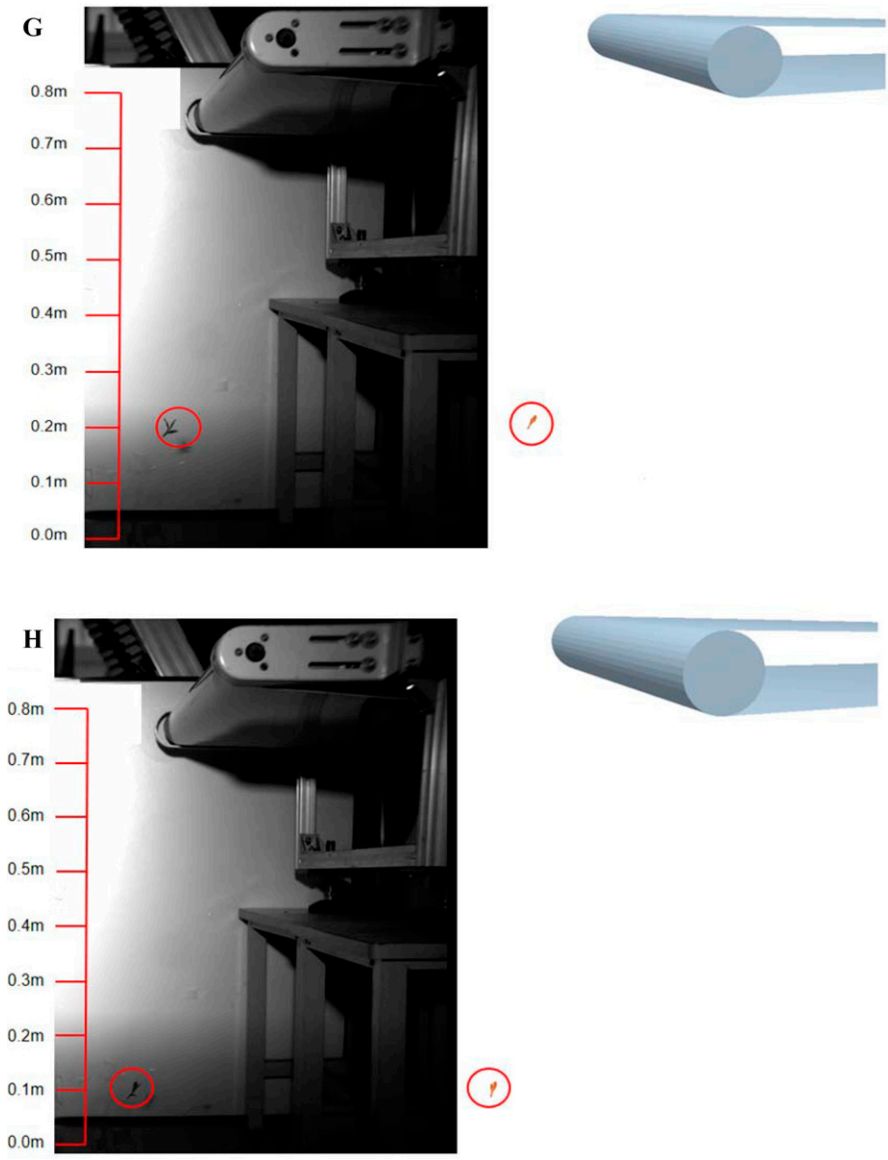

Fig. 5. (*Continued*)

the fresh tea leaves: if the leaf faces up, it was labeled "fresh tea leaf A"; leaves that face right were marked "fresh tea leaf B"; leaves facing down were marked as "fresh tea leaf C"; and leaves facing left were labeled "fresh tea leaf D." Among these, the motion characteristics of fresh tea leaf A were analyzed in simulation and test verification, and the motion characteristics of only fresh tea leaves B, C, and D are analyzed in this section. The movement marks of fresh tea leaves fall can be divided into rotation around the stalk axis of fresh tea leaves and rotation around the middle part of fresh tea leaves, as shown in Fig. 6

Analysis of falling motion characteristics of fresh tea leaf B. Figure 7 shows the falling motion patterns of fresh tea leaf B at different distances from the ground. The falling morphology of fresh tea leaves at different distances from the ground is analyzed respectively. Starting from the right side of the transmission belt facing the fresh tea leaves, the distance between the fresh tea leaves and the ground is 65 cm in Fig. 7A. The leaves rotate around their middle and rotate from the right side to the upside. Figure 7B shows leaves 55 cm from the ground. At this time, the leaves are in the trend of a leaf upward and stalk downward movement, reaching a vertical orientation to the ground. Compared with Fig. 7A, the leaves rotate around the stalk axis and the middle part of the leaves. Figure 7C is 45 cm from the ground; at this time, the fresh tea leaves have a tendency to rotate around their middle, and, compared with Fig. 7B, the leaves have an obvious rotation pattern around the stalk axis. Figure 7D is 35 cm from the ground. At this time, the leaf movement tends to tilt to the right, and the leaves have a tendency to rotate around the stalk axis. Figure 7E is 20 cm from the ground, where the fresh tea leaves are inclined to the right. Compared with Fig. 7D, the leaves rotate around the stalk axis and the middle part of the leaves. Figure 7F is 5 cm away from the ground. Compared with Fig. 7E, there is still an obvious trend of turning around the middle of leaves and moving around the stalk axis.

Given the preceding analysis, it was found that when the fresh tea leaves fall in this position, they rotate around the middle part of the leaves and rotate around the stem axis. In the process of falling, when the fresh tea leaves are vertically downward, they gradually rotate around the middle part of the leaves and rotate around the stem axis, finally falling to the ground with the leaves facing the right side of the belt.

Analysis of falling motion characteristics of fresh tea leaf C. Figure 8 shows the movement morphology of fresh tea leaves marked "tea leaf C" at different heights from the ground during the falling process. Figure 8A shows that the leaves move downward from the transport belt at a distance of 65 cm from the ground, turn in the air, and are inclined to the left. Figure 8B is 55 cm from the ground, at which time the leaves are in a vertical falling state. Compared with Fig. 8A, the leaves rotate

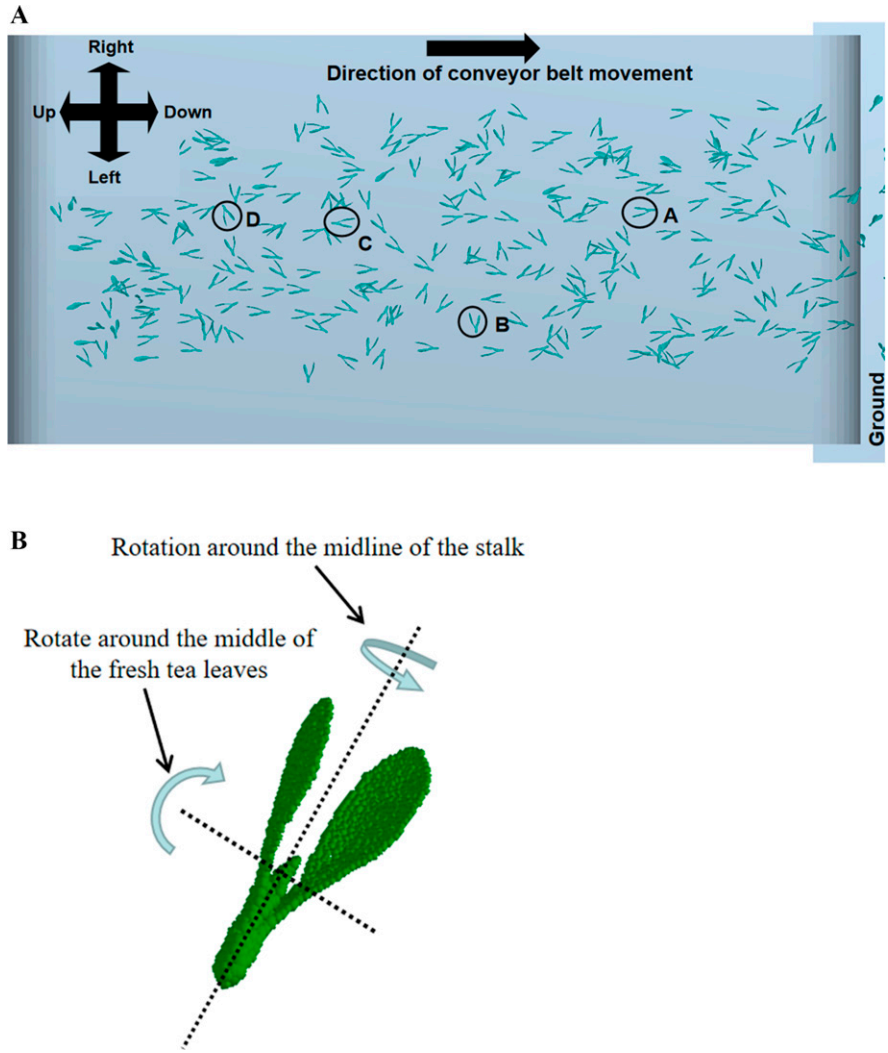

Fig. 6. The position and movement mode of tea fresh leaf transport belt. (**A**) Different forms of tea leaves on the transmission belt, including A/B/C/D four forms. (**B**) There are two motion states of fresh tea leaves in the falling process, including rotation around the axis of the tea stem and rotation around the middle line of the tea.

around the stalk axis and around the middle part of the leaves. Figure 8C is 45 cm from the ground. Compared with Fig. 8B, the fresh tea leaves continue to rotate around the stalk axis and rotate around the middle of the leaves, and the leaves have tilted from the vertical position to the right. Figure 8D is 35 cm away from the ground, where the leaves are parallel to the ground and continue to turn. Figure 8E is 20 cm away from the ground, at which time the leaves are oriented toward the ground. Figure 8F is 5 cm from the ground, where the fresh tea leaves are still facing the ground. Compared with Fig. 8E, there is only minor rotation of the leaves around the stalk axis.

In conclusion, the falling motion pattern of the transmission belt marked "fresh tea leaf C" mainly rotates around the stalk axis and around the middle part of the leaf. Within the fixed distance in this study, the fresh tea leaves placed at this position rotate 360° around the middle part of the leaf, and their falling patterns are different at different distances from the ground.

Analysis of falling motion characteristics of fresh tea leaf D. Figure 9 shows the movement patterns of fresh tea leaves marked "tea leaf D" at different heights from the ground during the falling process. Figure 9A is 75 cm from the ground, where the leaves fall behind the transport belt and rotate around the middle of the leaves; the rotation trend is leaves facing upward. Figure 9B is 65 cm from the ground, where the leaves are oriented downward vertically. Compared with Fig. 9A, there is an obvious rotation around the middle of the leaves. Figure 9C is 55 cm from the ground. Compared with Fig. 9B, the leaves rotate around the stalk axis and around the middle of the leaf. Figure 9D is 30 cm from the ground, where the leaves are moving at an angle parallel to the ground. Compared with Fig. 9C, the rotation around the stem axis and the rotation around the middle of the fresh tea leaves also occur. Figure 9E is 15 cm from the ground; the leaves are parallel to the ground. Figure 9F is 5 cm from the ground, and the running form of the leaves is similar to Fig. 9E, parallel to the ground.

In conclusion, the falling motion pattern of the transmission belt marked "fresh tea leaves D" is also mainly rotated around the stalk axis and around the middle part of the leaves, but the fresh tea leaves in the transmission belt arrangement form reach the vertical and ground state earlier than in the other arrangements.

Conclusion

In this study, inverse modeling and particle filling of "one bud and two leaves" of fresh tea leaves were carried out, and the falling motion model of the bud and leaves was established through EDEM discrete element software. The falling pattern of leaves was photographed with a high-speed camera to verify the simulation results. By adjusting parameters and optimizing the model, the discrete element model with greater than 97% agreement between simulation and test was finally obtained. The falling motion patterns of fresh tea leaves in different places (labeled A, B, C, and D) were analyzed. It was concluded that fresh tea leaves rotate around the stalk axis and the middle part of leaves during the falling process. Among them, fresh tea leaf A was 45 cm from the ground, fresh tea leaf B was 55 cm away from the ground, fresh tea leaf C was 55 cm from the

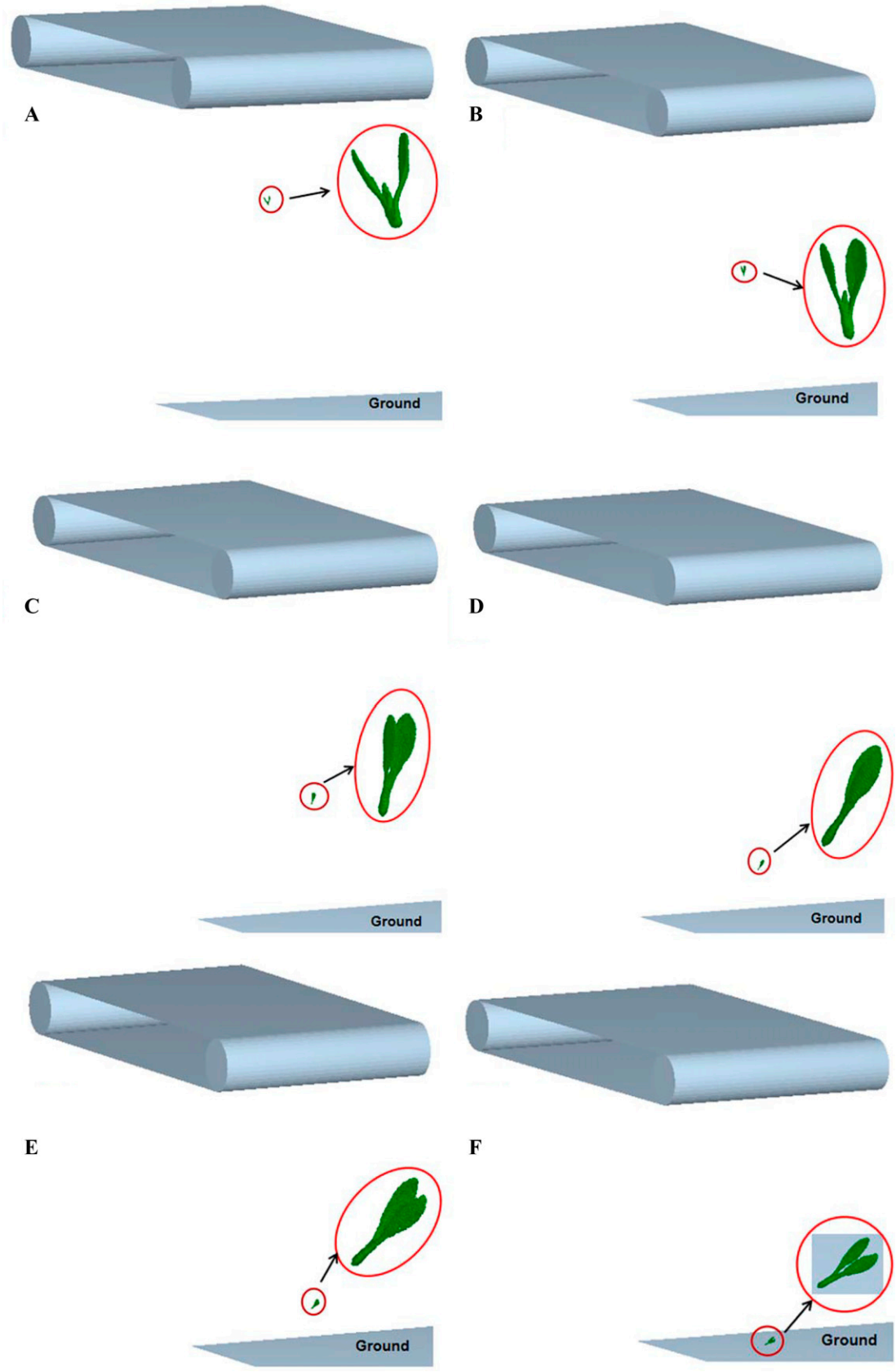

Fig. 7. The movement pattern of fresh tea leaf B at different distances from the ground. Fresh tea leaves fall from the conveyor belt at 0.65, 0.55, 0.45, 0.35, 0.20, and 0.05 m from the ground.

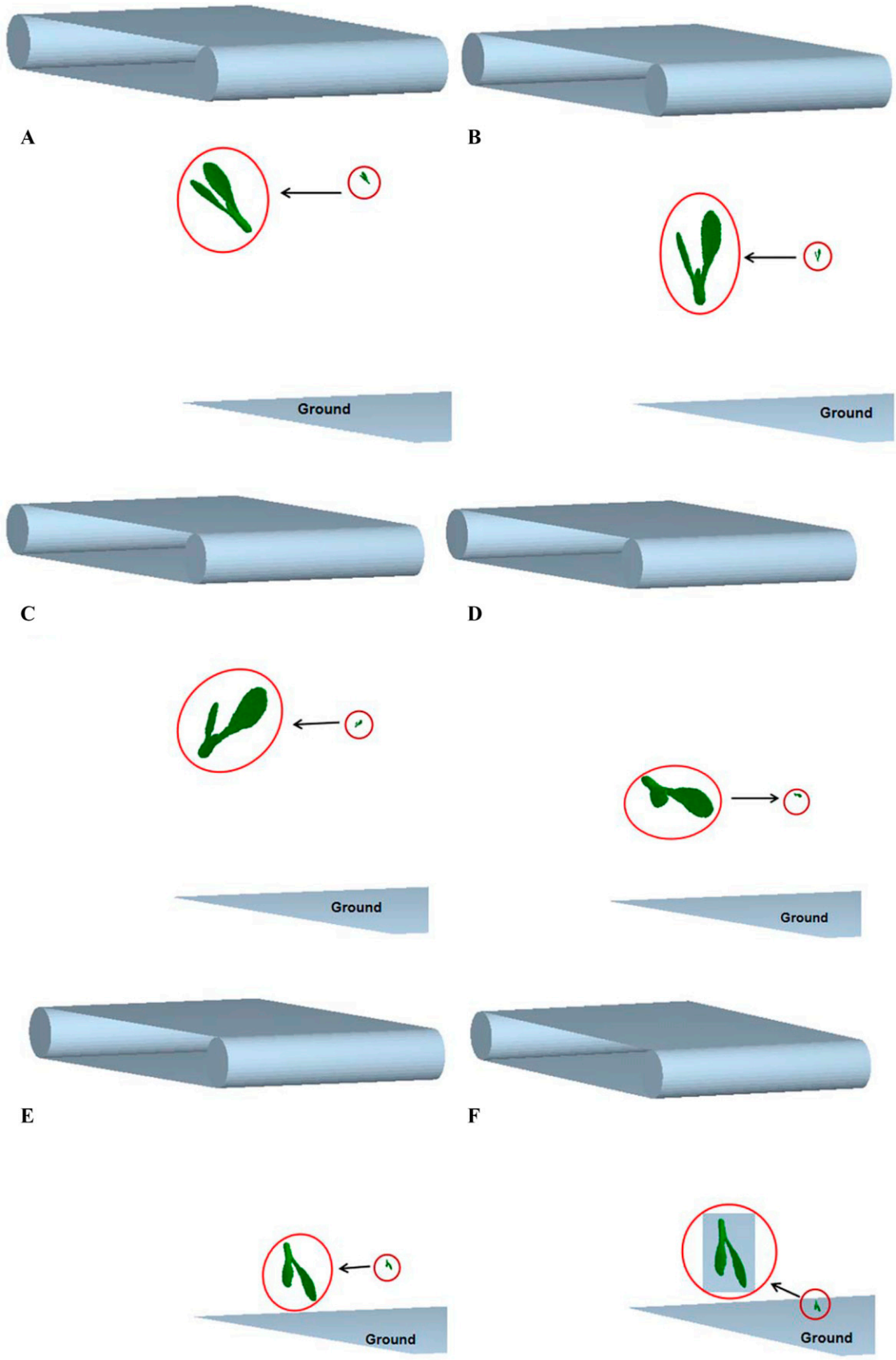

Fig. 8. The movement pattern of fresh tea leaf C at a different distance from the ground. Fresh tea leaves fall from the conveyor belt at 0.65, 0.55, 0.45, 0.35, 0.20, and 0.05 m from the ground.

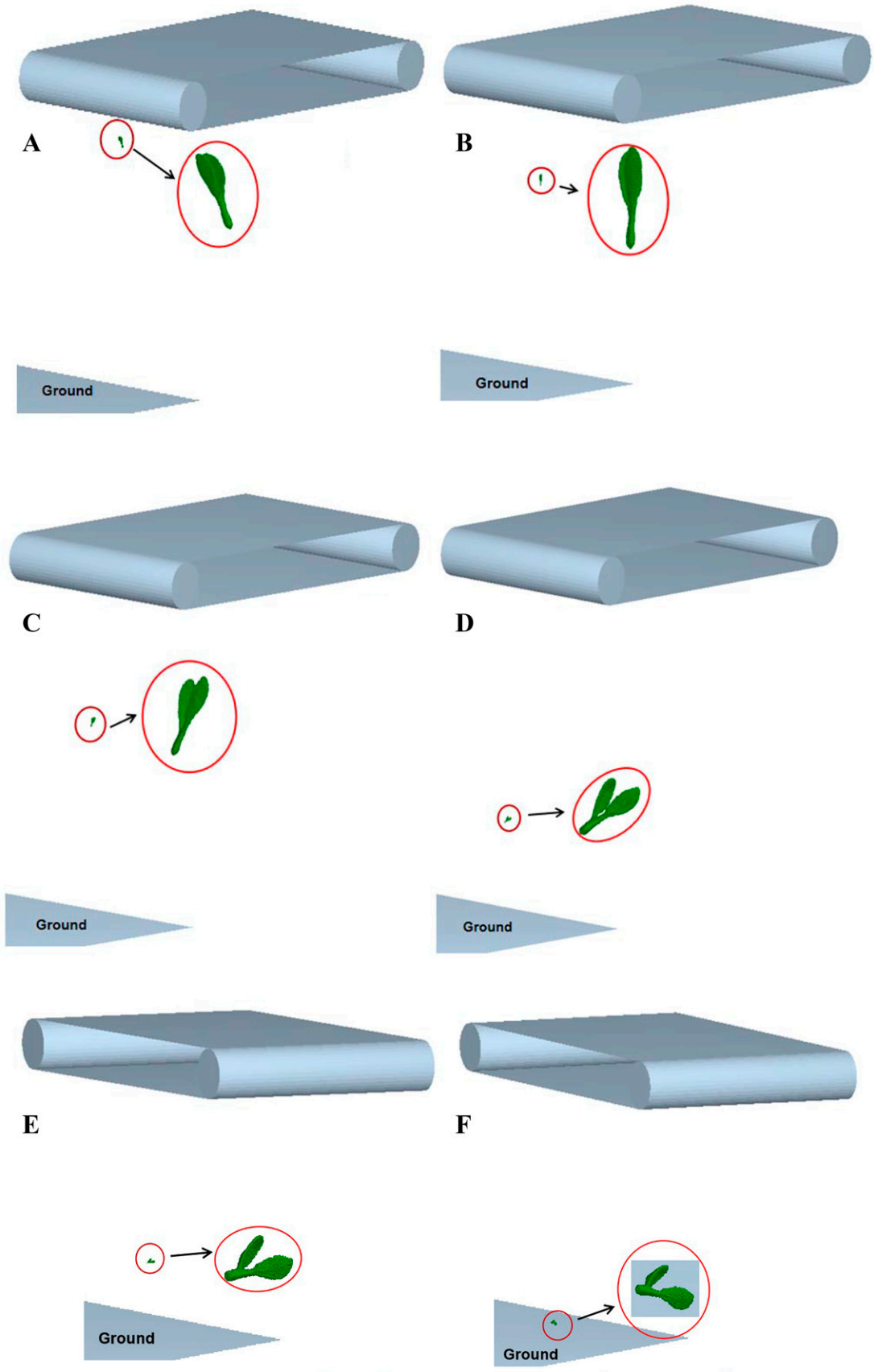

Fig. 9. The movement pattern of fresh tea leaf D at different distances from the ground. Fresh tea leaves fall from the conveyor belt at 0.75, 0.65, 0.55, 0.30, 0.15, and 0.05 m from the ground.

ground, and fresh tea leaf D was 65 cm away from the ground.

References Cited

Di Renzo A, Di Maio FP. 2004. Comparison of contact-force models for the simulation of collisions in DEM-based granular flow codes. Chem Eng Sci. 59:525–541. https://doi.org/10.1016/Jj.ces.2003.09.037.

Dong S, Yuan Z-H, Gu C. 2017. Research on intelligent agricultural machinery control platform based on multi-discipline technology integration. Nongye Gongcheng Xuebao (Beijing). 33(8):1–11. https://doi.org/10.11975/j.issn.1002-6819.2017.08.001.

Li B, Li W-N, Bai B-X. 2019. Study on screening rate of fresh tea leaf classifier based on EDEM. Tea Sci. 39(4):484–494. http://www.cnki.com.cn/Article/CJFDTotal-CYKK201904015.htm.

Li J-G, Liu M-X, Zou L-L. 2021. Discrete element modeling method and experimental verification of spinach main-root. Nong-ji-hua Yanjiu. 43(8):181–185, 191. https://www.doc88.com/p-51899826860242.html.

Li Y-K, Sun Y-Z, Bai X-W. 2015. Discrete element simulation of single mold hole densification molding process of corn stalk powder. Nongye Gongcheng Xuebao (Beijing). 31(20):212–217. https://doi.org/10.11975/j.issn.1002-6819.2015.20.030.

Liao Y-T, Liao Q-X, Zhou Y. 2020. Parameters calibration of discrete element model of fodder rape crop harvest in the bolting stage. Trans Chinese Soc Agric Machine. 51(6):73–82. https://doi.org/10.6041/j.issn.1000-1298.2020.06.008.

Liu W-Z, He J, Li H-W. 2018. Calibration of simulation parameters for potato mini tuber based on EDEM. Nongye Jixie Xuebao. 49(5):125–135. https://doi.org/10.6041/j.issn.1000-1298.2018.05.014.

Lu F-Y, Ma X, Tan S-Y. 2018. Simulative calibration and experiment on main contact parameters of discrete elements for rice bud seeds. Trans Chinese Soc Agric Machine. 49(2):93–99. https://doi.org/10.6041/j.issn.1000-1298.2018.012.

Lv H-V, Wu C-Y, Tu Z. 2022. Optimization of classification parameters of vibrating classifier for fresh tea leaves by the machine based on EDEM. Tea Sci. 42(1):120–130. https://www.cnki.net/.

Oka Y-I, Okamura K, Yoshida T. 2005. Practical estimation of erosion damage caused by solid particle impact: Part 1: Effects of impact parameters on a predictive equation. Wear. 259(1–6):95–101. https://doi.org/10.1016/j.wear.2005.01.039.

Peng F, Wang H-Y, Fang F. 2018. Calibration of discrete element model parameters for pellet feed based on injected section method. Trans Chinese Soc Agricultural Machine. 49(4):140–147. https://doi.org/10.6041/j.issn.1000-1298.2018.04.016.

Potyondy DO, Cundall PA. 2004. A bonded-particle model for rock. Int J Rock Mech Min Sci. 41(8):1329–1364. https://doi.org/10.1016/j.ijrmms.2004.09.011.

Qi X-Y, Zhou Z-Y, Yang C, Luo X-W, Gu X-Y, Zang Y, Liu W-L. 2016. Design and experiment of key parts of pneumatic variable-rate fertilizer applicator for rice product. Nongye Gongcheng Xuebao (Beijing). 32(6):20–26. https://doi.org/10.11975/j.issn.1002-6819.2016.06.003.

Sakaguchi H. 1993. Plugging of the flow of granular materials during the discharge from a silo. Int J Mod Physics B. 07(09n10):1949–1963. https://doi.org/10.1142/S0217979293002705.

Tang X-L, Li W-C, Fan Q-Y. 2015. Research on the classification technology and the grading equipment of machine-plucking fresh leaves. Chinese Tea Processing. 2:5–8.

Wang L-J, Li Y, Liang C. 2015. Motion law of maize mixture in cross air-and-screen cleaning device. Nongye Jixie Xuebao. 46(9):122–127.

Wang M-M, Wang W-Z, Yang L-Q. 2018. Research of discrete element modeling method of maize kernel based on EDEM. J Henan Agric Univ. 52(1):80–84, 103. http://xuebao.jlu.edu.cn/gxb/article/2018/1671-5497-48-5-1537.html.

Wang R-Y. 2020. Numerical calculation of gas-solid coupling of flexible flake materials and experimental study on sorting device for fresh tea leaves by machine. Zhejiang Sci-Tech University, Hangzhou, Zhejiang. https://kns.cnki.net/kns8/defaultresult/index

Wang X-L, Hu H, Wang Q-J. 2017. The calibration method of soil contact characteristic parameters is based on DEM theory. Trans Chinese Soc Agric Machine 48(12):78–85. https://doi.org/10.6041/j.issn.1000-1298.2017.12.009.

Wang W-W, Cai D-Y, Xie J-J, Zhang C-L, Liu L-C, Chen L-Q. 2021. Parameter calibration of discrete element model for compact molding of corn stalk powder. Chinese J Agric Machine. 52(3):127–134. https://doi.org/10.6041/j.issn.1000-1298.2021.03.013.

Wen X-Y, Yuan H-F, Wang G, Jia H-L. 2020. The calibration method of friction coefficient of granular fertilizer by discrete element simulation. Nongye Jixie Xuebao. 51(2):115–122, 142. https://doi.org/10.6041/j.issn.1000-1298.2020.02.013.

Xing H, Zang Y, Wang Z-M. 2019. Design and parameter optimization of rice pneumatic seeding metering device with adjustable seeding rate. Nongye Gongcheng Xuebao (Beijing). 35(4):20–28. http://www.doc88.com/p-9304465564048.html.

Yuan J-B, Li H, Wu C-Y, Qi X-D, Shi X-X, Li C. 2018. Study on apace particle modeling of rice grain basis on the discrete element method. Nanjing Nongye Daxue Xuebao. 41(6):1151–1158. https://doi.org/10.7685/jnau.201801004.